ASSESSMENT OF HAZARD TREE/SNAG DETECTION USING DRONE-BASED, MULTI-SPECTRAL SENSORS

by

Tyler Steinberg

FACULTY OF NATURAL RESOURCES MANAGEMENT
LAKEHEAD UNIVERSITY
THUNDER BAY, ONTARIO

April 2022

ASSESSMENT OF HAZARD TREE/SNAG TREE DETECTION USING DRONE-BASED, MULTI-SPECTRAL SENSORS

by

Tyler Steinberg

An Undergraduate Thesis Submitted in
Partial Fulfillment of the Requirements for the
Degree of Honours Bachelor of Science in Forestry

Faculty of Natural Resources Management
Lakehead University
April 2022

_____	_____
Ryan Wilkie	Colin Filliter
Major Advisor	Second Reader

LIBRARY RIGHTS STATEMENT

In presenting this thesis in partial fulfillment of the requirements for the Honours Bachelor of Science in Forestry (HBScF) degree at Lakehead University in Thunder Bay, I agree that the University will make it freely available for inspection.

Signature: _____

Date: April 13, 2022

A CAUTION TO THE READER

This Honours Bachelor of Science in Forestry (HBScF) thesis has been through a semi-formal process of review and comment by at least two faculty members. It is made available for loan by the Faculty of Natural Resources Management for the purpose of advancing the practice of professional and scientific forestry.

The reader should be aware that opinions and conclusions expressed in this document are those of the student and do not necessarily reflect the opinions of the thesis supervisor, the faculty or Lakehead University.

ABSTRACT

Steinberg, T. 2022. Assessment of hazard tree/snag detection using drone-based, multi-spectral sensors. *Natural Resources Management.* Lakehead University. 42 pp.

Keywords: drone, hazard tree, multi-spectral, sensor, snag, vegetation indices

Snags are an integral component of forest ecosystems as they provide habitat for a number of different species and add complexity to vertical forest structure. However, snags also may pose as potential hazards to people and property. Efficient and effective methods to locate and assess snags/hazard trees holds value to resource and conservation managers. This study aimed to assess the feasibility of using drone-based, multi-spectral sensors for detecting snags/hazard trees. The methods used in the study included an autonomous drone flight over the study areas, orthomosaic processing, object-based image analysis (OBIA), an accuracy assessment, and a field ground truth. The results provided sufficient evidence of drone-based, multi-spectral sensors being effective at detecting snags/hazard trees. However, the methods used in this study were found to only be accurate at detecting high quality/hazard snags. Segmentation parameters had a significant impact on the degree of quality/hazard of snag that the algorithm could detect. The orthomosaic classification was considered as highly accurate with an overall accuracy of 93.4%. Resource and conservation managers can effectively use the methods from this study for a variety of applications that aim to promote biodiversity and/or minimize public hazards.

CONTENTS

TABLES

FIGURES

ACKNOWLEDGEMENTS

I thank Lakehead University for supplying the necessary tools and equipment, Ryan Wilkie for assisting me as my thesis supervisor, Colin Filliter for being my second reader, and Ryan Mackett from the Lakehead Region Conservation Authority (LRCA) for providing permission to fly over and study the Cascades Conservation Area.

1.0 INTRODUCTION

As land management strategies become progressively more innovated, the use of drones or Remotely Piloted Aircraft Systems (RPAS) is becoming significantly more popular for a plethora of applications. An area of land management that has not been extensively tested for drone applicability is snag/hazard tree detection. With the high ecological significance of snags, and their accompanying potential hazards to people or property, improving known detection methods is important. This thesis aims to test the accuracy of snag tree detection using a MicaSense dual, 10-band multispectral sensor attached to a drone. The results of this study can potentially open up a new opportunity for land managers to detect snags/hazard trees more efficiently and accurately, allowing for more effective management decisions to be made.

Trees designated as snags or hazard trees will inevitably exist in any aging forest as some trees get sick and/or die off over time (Angers et al. 2010). However, when the proximity of these hazardous trees become close to frequent human activity or property, they must be assessed for management decisions that mitigate all possibilities of injury or property damage (Smiley et al. 2000). The method used most frequently for hazard tree detection and assessment is currently visual inspection, which can involve an expensive and laborious process when looking at large areas or long trail networks (Fink 2009). Using drones to detect these hazard trees more efficiently could reduce costs of detection and allow for management decisions to be made quickly, lowering potential risks.

Knowledge of snag locations in harvest blocks is also very beneficial to forest resource managers. Snags are an integral component of forests with great significance to animal habitats, as they increase vertical, structural complexity (Thomas et al. 1979). A variety of small mammals, birds, invertebrates, fungi, mosses, and lichens have several uses for snags (Thomas et al. 1979). Many of these species require accessibility to dead standing timber for their general or specialized habitat niches (Thomas et al. 1979). To ensure these habitat standards are maintained, a minimum number of snags per hectare must remain in a cutblock proceeding harvest (Thomas et al. 1979). Thus, forest resource managers must effectively determine whether a sufficient number of snags are present in a block or not prior to harvest to maintain the previous habitat niche. Applying remote imagery pre-harvest would allow for a manager to get a general view of the stand for visual assessment. However, the addition of multispectral sensors to the remote imagery can provide more detailed results to allow for more effective management decisions (Minařík and Langhammer 2016).

1.1 OBJECTIVE

The selected study area was the Cascades Conservation Area, which is a popular outdoor recreational area in Thunder Bay owned by the Lakehead Region Conservation Authority (LRCA). The LRCA is responsible for the sustainable management of watershed resources, with jurisdiction over ~2,719 km^2 around the Thunder Bay region, and 8 conservation areas including the Cascades (LRCA n.d.). Due to the frequent use of these conservation areas for

recreational purposes, it is crucial to ensure the trees do not pose a risk to visitors. Thus, hazard tree assessments must be conducted relatively often. Being able to use multispectral imagery from the MicaSense dual 10-band sensor would potentially allow for more of the conservation area to be assessed quicker and hazardous trees that are difficult to assess from the ground would be detected easier. Using the several spectral bands provided by the sensor for calculating zonal statistics, vegetation indices, and classification using QGIS are expected to effectively detect these dead standing trees. The objective of this study is to see if these methods are feasible.

1.2 HYPOTHESIS

Based on the success of similar drone-based multispectral applications (Minařík and Langhammer 2016; Dash et al. 2018), it is hypothesized that the drone-based MicaSense dual 10-band sensor can feasibly be applied to snag/hazard tree detection. The alternative hypothesis is that the application of drone-based MicaSense dual 10-band sensors is not a feasible method for snag/hazard tree detection. These hypotheses are also dependent on all classifications being performed using QGIS.

2.0 LITERATURE REVIEW

2.1 DRONES IN FORESTRY

Remote sensing techniques provide forest managers with competitive advantages that allow for an increased detail of sustainable management factors such as forest structure, composition, volumes, or growth to be assessed (Banu et al. 2016). Due to the technological innovations and advancements of sensors and computers, the main data collection method has shifted from being aerial photography to satellite imagery, as several forest indices could then be calculated to more accurately estimate data (Banu et al. 2016). However, acknowledgment of the imagery scale that is necessary for the type of data collection is important, as aerial photographs will be more suitable for smaller scale details, and vice versa (Sedykh 1995). Drones have a great potential of providing the optimal remote sensing data for high spatial resolution applications where aerial photography and satellite imagery would not be suitable (Banu et al. 2016). The broad applicability, low-costs, and high-resolution outputs of drone data collection are key factors to its success in filling in the remote sensing gap between manned aerial photography and satellite imagery (Tang and Shao 2015).

2.1.1 APPLICATIONS

Koh and Wich (2012) demonstrated the applicability of inexpensive drone technology for surveying and mapping forests and biodiversity. A low-cost drone (<$2,000) was developed with capabilities of a ~25-minute flight time with over a ~15 km maximum travel distance. The drone also had the ability to capture

video with a 1080p resolution and acquire aerial images with a pixel resolution of <10cm. Several test flights over various study sites in tropical landscapes (Aras Napal, Sumatra, Indonesia), revealed that the prototype drone was an effective tool for collecting remote sensing data on land mapping, detection of human activities, and biodiversity. The data recorded in this study is significant evidence that drones can be a highly valuable, inexpensive tool for data collection where high-resolution is required.

Satellite imagery has been a sufficient remote sensing tool for collecting data on forest gap dynamics, however it lacks the ability of obtaining accurate results for small, localized disturbances such as blow-down (Frolking et al. 2009; Getzin et al. 2012). Especially in forest management, knowledge of small forest gaps can be evidential of key diversity and productivity factors (Tang and Shao 2015). Getzin et al. (2012) deployed an autonomous Carolo P200 drone to test whether or not drones could accurately detect small forest gaps in temperate forests. The drone was flown at an altitude of 250 m, capturing 1 m spatial resolution images (Getzin et al. 2012). The results of Getzin et al. (2012) concluded that high-resolution imagery obtained from drone's can be successfully utilized for assessing biodiversity using gap dynamics.

Forest canopy height measurements were historically all estimated using photogrammetric methodology and ground surveys (Tang and Shao 2015). The use of these methods for canopy height data collection has become sparse in recent years, as more advanced remote sensing technology, such as Light Detection and Ranging (LiDAR), has been recognized as a superior measurement tool (Lefsky et al. 2002). With the major innovations made to

LiDAR equipment to make it lighter and require less power, the adaptability with drone technology has become apparent (Risbøl and Gustavsen 2018). Although LiDAR is not yet globally accessible, studies by Lisein et al. (2013), Zarco-Tejada et al. (2014), and Dandois and Ellis (2013) have displayed that lower-cost, alternative methods such as measuring canopy heights using drones without LiDAR can be successfully accomplished.

Wildfires are common natural disturbances that promote succession in forests (Bergeron et al. 1998), though they also have potential to pose risks to human health and safety, property, and ecological variables (Samiappan et al. 2019). To ensure wildfires are being effectively managed, frequent and reliable surveying is required to track the spread and intensity of fires (Allison et al. 2016). As satellite imagery does not provide high enough resolution images to detect small local fires, and manned aircrafts can be costly and present risk to crew members, drones provide a solution with higher temporal and spatial resolution, at lower costs and risk (Tang and Shao 2015). Drones can also be utilized for post-fire analysis, which is evident in the success of the Samiappan et al. (2019) study, where recently charred areas were accurately mapped, and vegetation recovery and damage analysis was feasible using an autonomous drone equipped with a MicaSense RedEdge 5-band multispectral sensor.

Drones have also been effectively implemented in the aid of intensive forest management strategies with support in estimating key variables such as tree/stand vigour, density control, brush control, and more (Tang and Shao 2015). Since each wavelength range is reflected off of foliage at varying proportions, differences in reflectance patterns can be used to determine the

health of stands or individual trees (Slaton et al. 2001). Previous studies have validated that the reflectance of near-infrared (NIR) is reduced and the reflectance of red is increased in stressed vegetation when compared to healthy vegetation (Felderhof and Gillieson 2011; Dash et al. 2018). With the addition of multispectral sensors to drones, vegetation indices can be utilized to process imagery in a manner that detects forest characteristics that cannot be easily detected by the human eye (Mahajan and Bundel 2016).

Table 1 shows the flight parameters used for some of the previously mentioned drone application examples. Having reference to the flight parameters that were applied in several successful studies will allow for future interpretations of whether or not the results were likely to have been impacted by the flight parameters used in this study.

Table 1. Flight parameters used in previous successful drone studies.

Study	Platform/Sensor	Flying Height (m)	Overlap (%)
Koh and Wich (2012)	RGB Canon Camera and a GoPro	180	>50
Getzin et al. (2012)	High-resolution RGB camera	250	Undefined
Lisein et al. (2013)	Ricoh GR3 Camera adapted for NIR	225	75
Samiappan et al. (2019)	MicaSense RedEdge	305	X - 60 Y - 70
Dash et al. (2018)	MicaSense RedEdge 3	90	85

2.2 MICASENSE DUAL, 10-BAND MULTISPECTRAL SENSOR

While conventional multispectral sensors only provide 5 bands, the MicaSense dual sensor doubles the number of bands to 10 by combining the technology of the RedEdge-MX and RedEdge-MX Blue sensors (Pranga et al. 2021). The variety of 10 bands with supplemental green, red, and red-edge bands, offers substantially more spectral information on vegetation than that of traditional cameras (Pranga et al. 2021). A set range of wavelengths is designated for each band, Table 2, that can provide data for computational processing of vegetation indices (Assmann 2018). The utilization of vegetation indices provides more in-depth information on ecological variables like vegetation productivity and leaf area index (LAI), as various combinations of the provided spectral bands in Table 2 can be applied to individual applications to produce different visual representations of spatial area (Assmann 2018). A wider variety of spectral bands opens up opportunity for experimentation with a broader range of vegetation indices. However, many of the potential applications for the MicaSense dual sensor have yet to be explored due to its relatively new introduction to commercial use.

2.2.1 BANDS

Table 2. Corresponding center wavelengths and bandwidths for each MicaSense Dual sensor band.

Band Name	Center Wavelength (nm)	Bandwidth (nm)
Coastal Blue	444	28
Blue	475	32
Green	531	14
Green	560	27
Red	650	16
Red	668	14
Red Edge	705	10
Red Edge	717	12
Red Edge	740	18
Near IR	842	57

Source: MicaSense 2018

The most critical bands for analyzing the health of trees are the red, red edge and NIR bands (Xiao and McPherson 2005). The red edge bands are highly valuable, as they can provide details that may not be evident using the red bands in combination with the NIR band (Mutanga and Skidmore 2007). Red edge has also been found to be less affected by background soil and atmospheric affects (Darvishzadeh et al. 2009). Previous studies have shown success in applying red edge bands to effectively make estimations of chlorophyll concentration, biomass, and LAI (Mutanga and Skidmore 2007). The

green bands are also required to be accounted for in remote sensing for tree health, though the data from them is not as valuable (Xiao and McPherson 2005).

2.2.2 VEGETATION INDICES

Over the last 30 years, there have been over 40 vegetation indices that have been publicly released, each calculating different parameters to generate various solution responses that enhance distinct forest aspects while minimizing others (Bannari et al. 2009). Traditionally, the Normalized Difference Vegetation Index (NDVI) is most commonly utilized for forest management activities, as it has successfully shown accuracy at detecting LAI, living biomass, and vegetation coverage (Purevdorj et al. 1998). Although there is major success behind the NDVI, it still has known limitations like soil background and atmospheric sensitivity (Xue and Su 2017). Thus, more vegetation indices were developed to remediate these issues, such as the soil-adjusted vegetation index (SAVI), transformed soil-adjusted vegetation index (TSAVI), atmospherically resistant vegetation index (ARVI), and the modified soil-adjusted vegetation index (MSAVI) (Rondeaux et al. 1996). Although the NDVI is the expected vegetation index to be used in this study, a review of other potentially effective vegetation indices is listed in Table 3.

Table 3. Practical vegetation indexes for examining vegetation health attributes.

Index	Formula	Reference
Normalized Difference Vegetation Index (NDVI)	$\frac{NIR - RED}{NIR + RED}$	Purevdorj et al. 1998
Soil-Adjusted Vegetation Index (SAVI)	$\frac{NIR - RED}{NIR + RED + L}(1 + L)$	Purevdorj et al. 1998
Transformed Soil-Adjusted Vegetation Index (TSAVI)	$\frac{a(NIR - aRED - b)}{(RED + aNIR - ab)}$	Purevdorj et al. 1998
Modified Soil-Adjusted Vegetation Index (MSAVI)	$\frac{2NIR + 1 - \sqrt{(2NIR + 1)^2 - 8(NIR - RED)}}{2}$	Purevdorj et al. 1998
Normalized Difference Red Edge index (NDRE)	$\frac{NIR - RED\ EDGE}{NIR + RED\ EDGE}$	Delegido et al. 2013

Source: Purevdorj et al. 1998; Delegido et al. 2013

2.2.3 APPLICATIONS

Isgró et al. (2021) successfully demonstrated the use of the MicaSense dual, 10-band multispectral sensor for monitoring water quality. To do this, the study sampled and analyzed various acidic and non-acidic water bodies. The DJI Matrice 210 V2 RTK was equipped with the MicaSense dual sensor for sampling of each water body. With a flying height of 120 m, 80% frontal overlap, and 75% side overlap, these parameters effectively captured images of each site that could be transformed into orthomosaics. The 10 different bands for

each image produced by the dual sensor allowed for each chemical element of significance to be analyzed for any spectral relationships with certain bands. Isgró et al. (2021) concluded that the application of the MicaSense dual sensor for modelling water quality was highly valuable, as chemical detection by element can be completed efficiently and accurately over large areas of water.

Fernández et al. (2020) utilized the Micasense dual sensor for detecting potato late blight at both the leaf and canopy level by analyzing the various red and red edge bands provided by the sensor. Having access to a variety of bands in several spectral regions was important due to the study focusing on the effects of the disease that are only visible in the red and NIR spectral regions. For detection, the methods included a support vector machine classifier on both reflectance values of the MicaSense dual sensor bands and on red-well position/red edge inflection point wavelengths. It was discovered that classification using the reflectance values of the MicaSense dual sensor was more accurate (~89% accuracy) at classifying the disease at both the canopy and leaf level.

2.3 ECOLOGICAL IMPORTANCE OF SNAGS

Standing dead timber, otherwise known as snags, are critical to animal habitat, as a variety of animals and insects utilize or depend on their existence for survival (Thomas et al. 1979). The variety of quantity, size, and quality in present snags is highly influential on the maximum amount of wildlife that can persist in a local habitat (Thomas et al. 1979). Furthermore, the abundance and distribution of snags can be used as a key variable for biodiversity and forest

health, as nutrient cycling, long-term carbon storage, and fungal and invertebrate life strategies are all strongly correlated with standing dead timber (Wing et al. 2015). Due to the significance of snags, many forest management methods and policies require land managers to ensure minimum densities or volumes of standing dead timber is stocked to maintain ecological characteristics (Pasher and King 2009).

Strong land stewardship is highly valued by the LRCA with their strategies including shoreline naturalization, stormwater management, invasive species management, and habitat enhancement (LRCA n.d.). Since snags have significant ecological importance, ensuring that natural quantities and qualities exist is a strategy for protecting and promoting key stewardship values (Thomas et al. 1979; LRCA n.d.). However, in the several conservation areas that the LRCA manages, snags can pose as risks to recreational visitors (LRCA n.d.). Thus, a balance of maintaining natural ecological features and public safety must be exhibited.

2.4 SNAGS AS HAZARD TREES

Although snags are a critical component of natural forests, they can also potentially pose as risks to human safety or property damage (Stereńczak et al. 2017). In outdoor recreational areas, especially in highly trafficked/touristed areas, a relatively high quantity of snags can be of concern for decades (Stereńczak et al. 2017). As it is in the best interest of tree owners and land managers to avoid all potential liabilities, due diligence is necessary (Fink 2009). Thus, understanding the location and condition of snags consistently and

systematically is crucial for taking preventative measures in these areas (Fink 2009). Currently, the LRCA's hazard tree program relies primarily on a ground-based professional visually detecting and inspecting potential hazard trees throughout each year (LRCA n.d.). Any trees deemed as hazards to the public are then removed to ensure safety for all visitors and property (LRCA n.d.)

3.0 MATERIALS AND METHODS

3.1 MATERIALS

The equipment used for collecting data included the following: a DJI Matrice 200 drone, a MicaSense Dual 10-band multispectral sensor, a Calibrated Reflectance Panel 2 (CRP 2), and a Garmin GPSMAP 64 SERIES. The software used for image mosaicing, classification, and analysis included the following: Agisoft Metashape 1.5.5.9097, QGIS 3.2 with the Orfeo toolbox, and ArcGIS Pro 2.9.

3.2 AREA OF STUDY

The flights and data collection for this study were executed in a popular recreational conservation area that is managed by the LRCA, the Cascades Conservation Area. With a very close proximity to the city of Thunder Bay, it attracts many recreational users to enjoy its outdoor features. The Cascades Conservation Area is 162 ha and offers a variety of trail networks (5.5 km) that run through the Boreal forest, while also promoting inclusivity by providing wheelchair accessibility for a portion of the trails (LRCA 2016). Furthermore, the trails link with a segment of the Current River which gives users the opportunity

to enjoy the river and its rapids in addition to its forest trail network (LRCA 2016).

The first study area is outlined in red in Figure 1. It is the forested area confined by the Forest trail, which is the most accessible trail that spans 775m through the conservation area (LRCA 2016). Due to the frequent use and high accessibility of this trail, it is critical to ensure that the chance of a hazard tree causing an injury or preventing accessibility is minimized. Also, the relatively small area within the Forest trail allows for data collection and analysis to be completed quicker and more accurately. Thus, the resulting parameterizations to effectively detect hazard trees in this smaller area can be attempted to be repeated on a larger area.

The second study area is outlined in dashed blue in Figure 1. It is the forested area confined by portions of the Forest, Link, Orange, and Blue trails. This area was used as the larger area to test the effective parameterization based on sampling in study area 1.

Figure 1. Selected study sites in the Cascades Conservation Area.

3.3 DATA COLLECTION

On October 1st, 2022, the DJI Matrice 200 was flown autonomously to prevent any chances of human flying errors. A flight path was set for each study area on the proprietary DJI tablet, with corresponding flight parameterizations (Table 4). These were then named and saved for any future flights. At the same time, the MicaSense dual sensor was equipped to the drone and successfully connected. After all of the flight parameters were inputted and the sensor was calibrated and connected, the drone was engaged and began its flight path while collecting images. It is important to note that an image of the CRP 2 was taken

before and after each flight to ensure that the sensors provide an accurate representation of the light conditions that existed at the time of flying. The drone, sensor, and CRP 2 used in this study can be seen in Figure 2.

Figure 2. DJI Matrice 200 equipped with the MicaSense dual sensor, accompanied by the CRP 2. The stand being studied is visible in the background, displaying the stand complexity and species mixtures.

Table 4. Flight parameters for both study areas.

Parameter	Value
Flying Height (m)	120
Frontal Overlap (%)	80
Side Overlap (%)	80

3.4 PROCESSING MICASENSE IMAGES ON AGISOFT METASHAPE

The images from the MicaSense Dual 10-band multispectral sensor were processed in Agisoft Metashape. This procedure began with importing all of the photos, including the reflectance calibration images, ensuring that the “Multi-camera system” data layout was selected. Next, the reflectance panel images were located and inputted into Calibrate Reflectance. The reflectance calibration was then run with the “use reflectance panels” and “use sun sensor” parameters toggled on to normalize any variable light conditions that existed during flight.

While the reflectance calibration data was being processing, the photo alignment process could take place. The photos were aligned with the parameters provided in Table 5. To improve the alignment accuracy, the Optimize Cameras option was opened, and the following parameters were toggled on: Fit f, Fit cx, cy, Fit k1, Fit k2, Fit k3, Fit b1, Fit b2, Fit p1, Fit p2.

Table 5. Parameters used for the Align Photos dialog.

Parameter	Value
Accuracy	High
Generic preselection	On
Reference preselection	On
Reset current alignment	Off
Key point limit	40,000
Tie point limit	4,000
Apply masks to	None
Adaptive camera model fitting	Off

To produce a more accurate surface model a Dense Point Cloud was generated using medium quality, aggressive depth filtering, and using the calculate point colours parameter. To further create an accurate surface, a Digital Elevation Model (DEM) was built using the parameters found in Table 6.

Table 6. Settings used for building the DEM.

Settings	Value
Type	Geographic
Reference System	WGS 84 (EPSG:4326)
Source Data	Dense cloud
Interpolation	Extrapolated
Point classes	All

The DEM generated in the previous step can then be used in building the orthomosaic. The parameters used are seen in Table 7.

Table 7. Settings used for building the orthomosaic.

Parameters	Value
Surface	DEM
Blending Mode	Mosaic (default)
Refine Seamlines	Off
Enable Hole Filling	On
Pixel size (X)	1.12226e-06
Pixel size (Y)	7.73278e-07

The resulting orthomosaic image was then exported and utilized for the following steps to perform an object-based image analysis (OBIA). All OBIA results were achieved using the Orfeo Toolbox (OTB) in QGIS.

3.5 OBIA IN QGIS

To begin, a new QGIS file was created with the orthomosaic image opened as a raster. The *segmentation* tool was then applied and involved trial and error to determine parameter values that best represented objects in the image, most specifically tree crowns. The values that were found to be most critical to change were the spatial radius, range radius, and minimum region size. The values used for these 3 parameters are shown in Table 8, while all other parameters were left as default.

Table 8. Changed values in the segmentation tool.

Parameters	Value
Spatial radius	25
Range radius	75
Minimum region size	500

The resulting segmentation vector was imported into QGIS and confirmed for accuracy of object identification. Once verified, the ground sampling process took place. This involved the creation of a new point layer including an integer field called “Classified”. Representative integers were associated with two different classes, 2 for “SNAG” and 1 for “NOT SNAG”. The “NOT SNAG” class

had 265 points distributed across the image while ensuring all surfaces that were not snags were encapsulated. The selection of “SNAG” samples was only made within study area 1, with 21 snags being selected in total.

The *zonal statistics* tool was then applied, while defining the segmentation results as the input vector data and using the default parameters. Once completed, the sample points were joined with the zonal statistics results using the *Join Attributes by Location* tool, while applying “Take attributes of the first matching feature only (one-to-one)” as the join type and discarding records that could not be joined.

Next, the *train vector classifier* tool was used with the joined layer as the input vector data. The field names for training features parameter was populated with the field names of the mean and standard deviation for each band, and the field containing the class data was defined. All other parameters were left as default.

The final tool used was the *vector classifier* tool with the zonal statistics results as the input vector data and the train vector classifier results as the model file. The same fields that were inputted in the previous step were also defined in the field names to be calculated parameter. The resulting vector was effectively classified and could be visualized.

3.6 ACCURACY ASSESSMENT IN ARCGIS PRO

The classified vector and original orthomosaic raster were both imported into a new ArcGIS Pro project. The create accuracy assessment points tool was then applied, defining the classified vector as the feature class data, “Classified”

as the target field, and using an equalized stratified random sampling strategy with 1000 total points. Once the randomized points had completed generating, the attribute table for the accuracy assessment points was opened. Each point was then individually viewed, and their respective ground truth field values were populated. During this process, the classified field was hidden to minimize any potential biases.

Finally, the compute confusion matrix tool was used with the accuracy points as the input data. The resulting confusion matrix table was generated within ArcGIS Pro, and then exported as an excel file using the table to excel tool.

3.7 FIELD GROUND TRUTH

To assess the accuracy of the drone-based snag detection, a field ground truth method was selected. On November 21, 2022, five healthy trees and five snags were randomly selected in each study area and their coordinates were recorded using a Garmin GPSMAP 64. For each individual stem's GPS data collection, the GPS was placed near the base of the tree while ensuring the antenna was positioned upright and not obstructed by vegetation.

After the data for all of the ground samples had been collected, the snag vector data was overlaid on the classified images to compare whether or not the snags found on the ground were detected by the classification method, or if healthy trees were misclassified. A comparative analysis could then be executed using the respective results.

4.0 RESULTS

4.1 SEGMENTATION

For the segmentation to be considered sufficient for the purposes of this study, it had to generate segments that best fit the shape and overall size of tree crowns. Figures 3 and 4 show the results of using the default segmentation parameters compared with the results of the selected segmentation trial respectively. It is evident that with the changed parameterization, the total number of segments significantly decreased, while segment sizes significantly increased. This produced segments that were more representative of the overall crowns rather than several segments making up each crown.

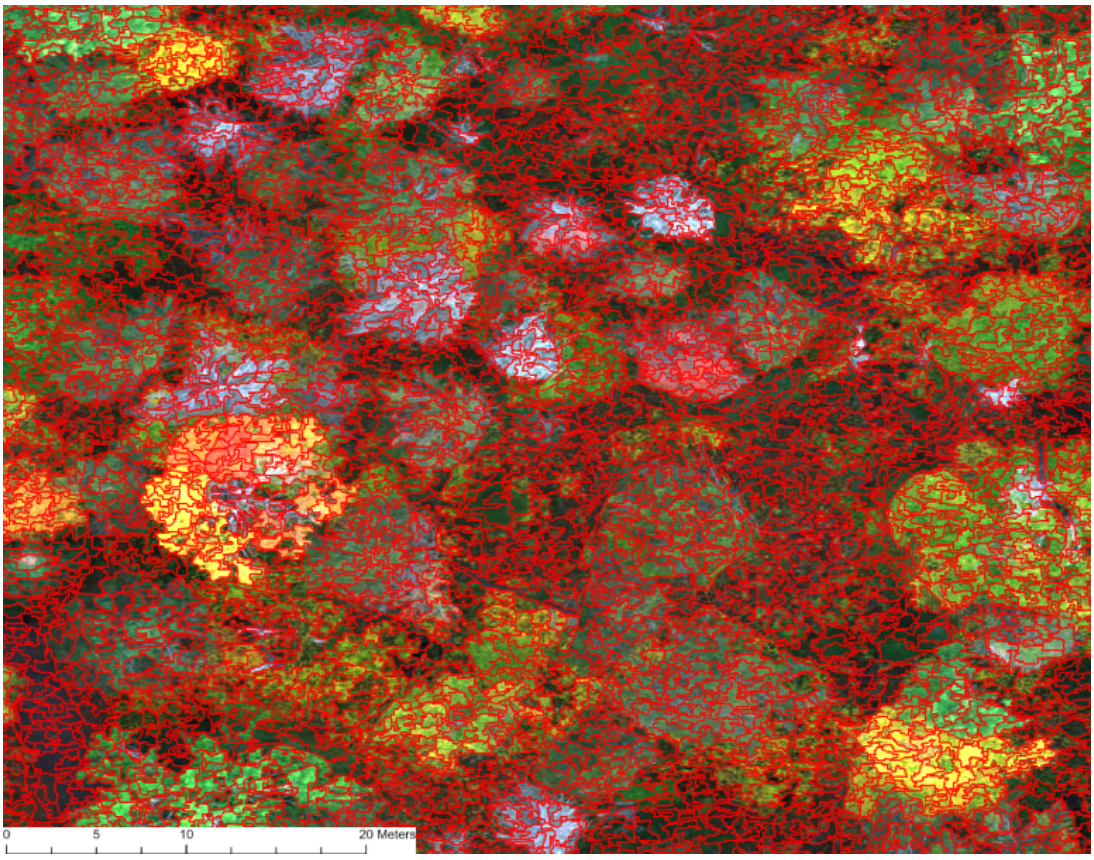

Figure 3. Segmentation results using default segmentation parameters. The segments can be seen as small in size and large in quantity.

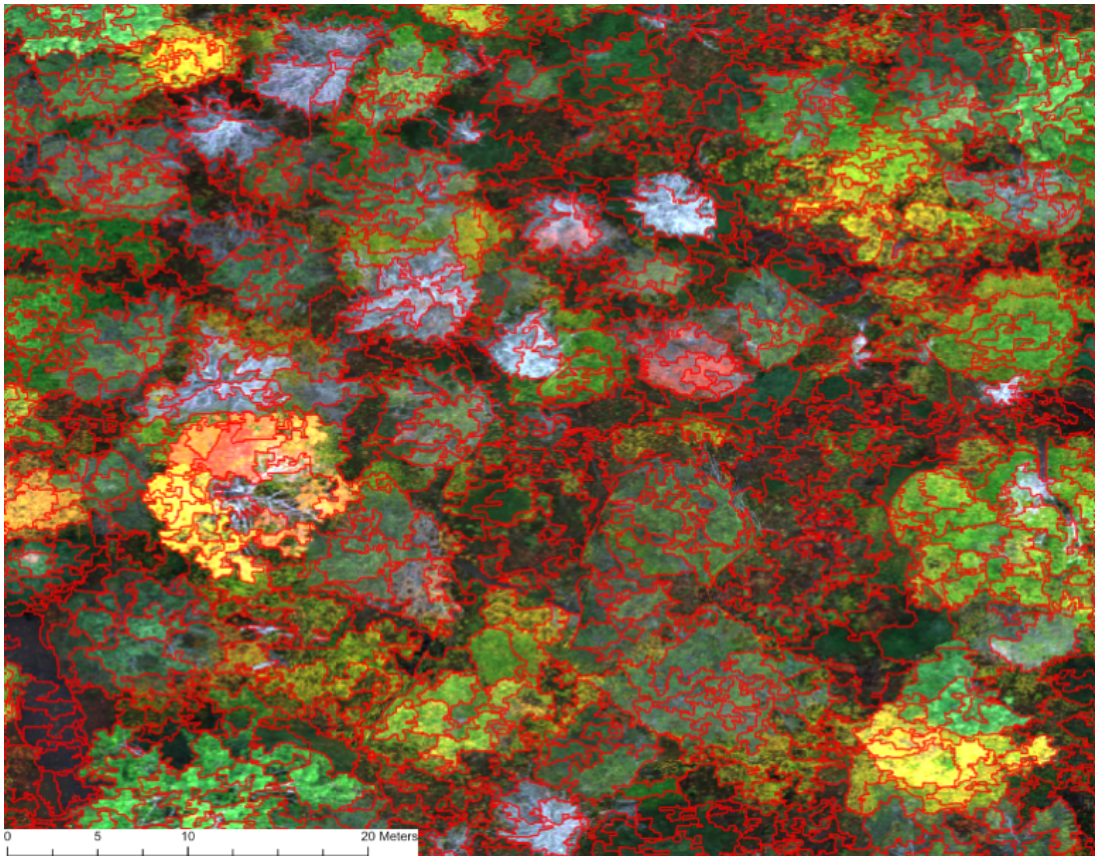

Figure 4. Segmentation results from the selected trial (refer to Table 8). Relative to the default segmentation, the segments are larger in size, better shaped to tree crowns, and fewer quantities exist.

4.2 CLASSIFICATION

Figure 5 shows the results of the snag classification at full scale, depicting that the algorithm has identified various snags throughout each study area (identified snags outlined in red). It can also be noticed there are some small clusters of snags that exist. Figures 6 and 7 shows the snag classification at a scale of 1:200 within study area 1 and study area 2 respectively. At this scale, the classification of individual standing dead stems can be viewed with more detail.

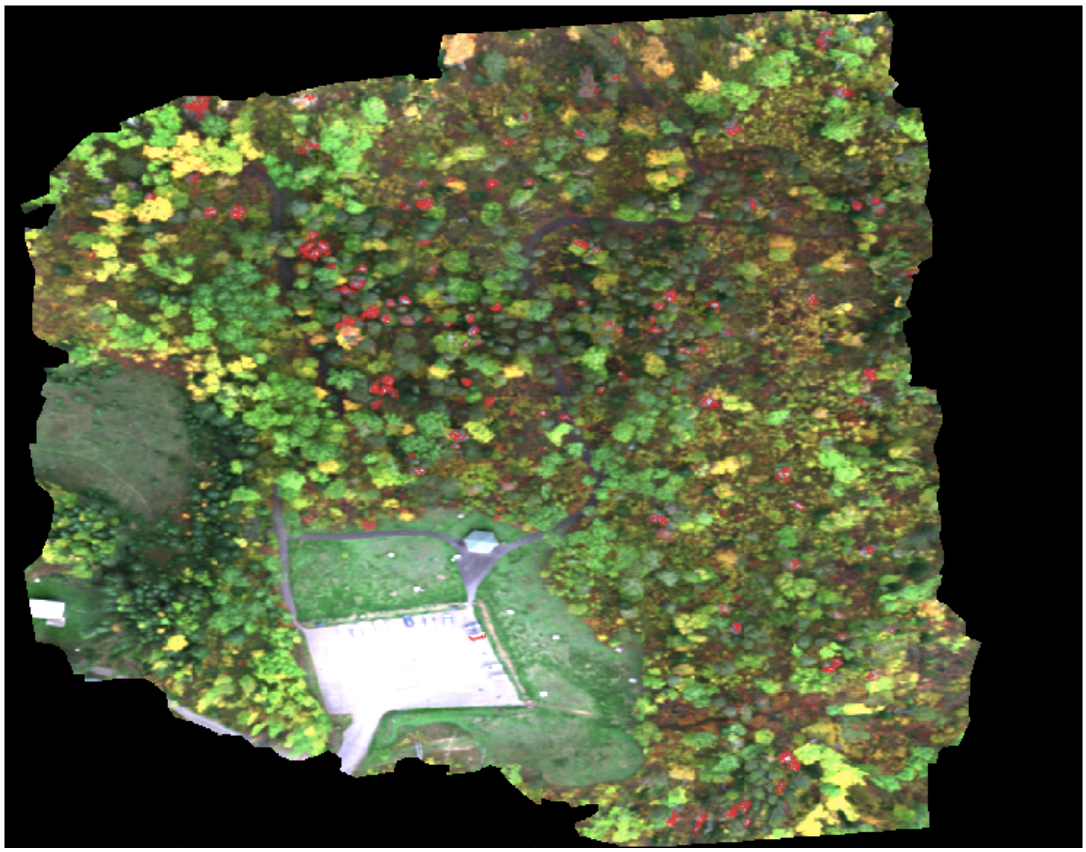

Figure 5. Snag classification at full scale.

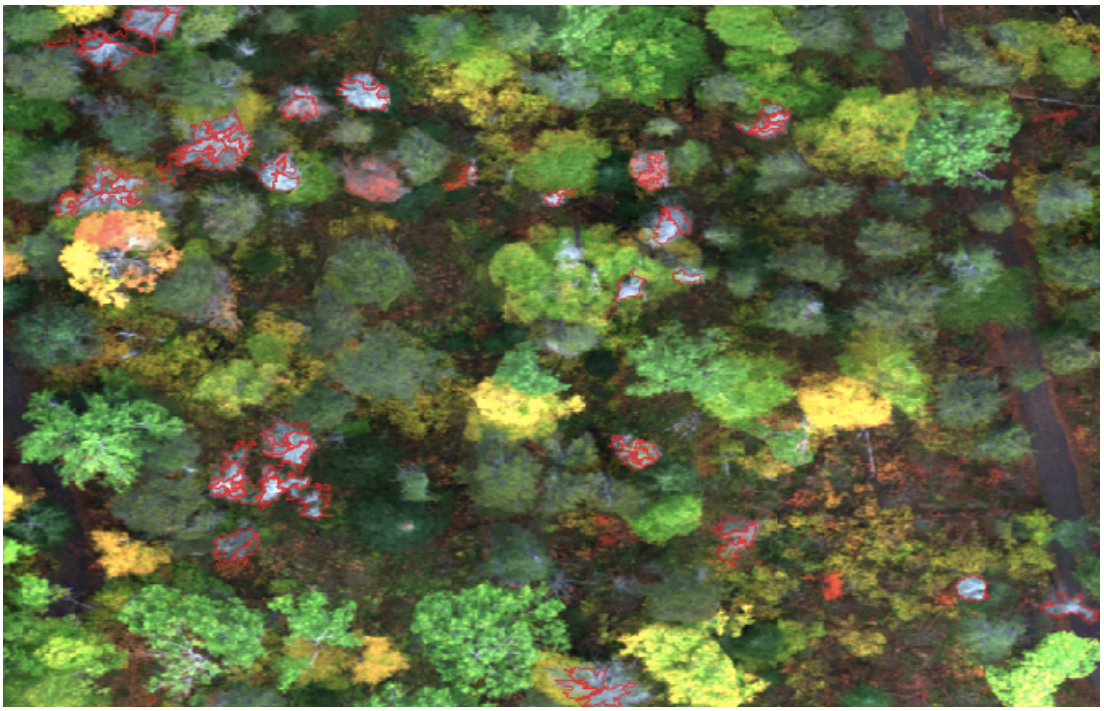

Figure 6. Snag classification at a scale of 1:200 in study area 1.

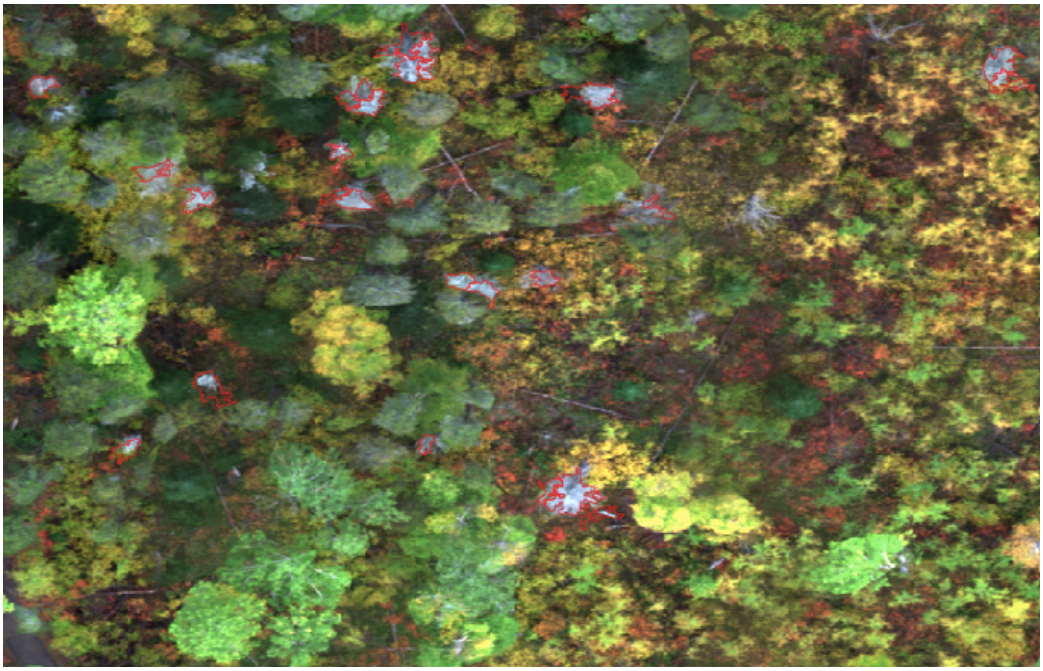

Figure 7. Snag classification at a scale of 1:200 in study area 2.

4.3 ACCURACY ASSESSMENT

As seen in Table 9, the minimum accuracy for all classes was 89% or more, with an overall accuracy of 93.4%. There was also a relatively high level of agreement in the data (Cohen 1960) with a kappa value of 0.87. In the “Not Snag” class, 11 objects were errors of commission and 55 were errors of omission. In the snag class, 55 objects were errors of commission and 11 were errors of omission.

Table 9. Confusion matrix for snag classification results.

ClassValue	Not Snag	Snag	Total	User Accuracy	Kappa
Not Snag	489	11	500	97.8%	
Snag	55	445	500	89.0%	
Total	544	456	1000		
Producer Accuracy	89.9%	97.6%		93.4%	
Kappa					0.87

4.4 FIELD GROUND TRUTH

Table 10 shows the results of the ground truth field sampling for study area 1 and study area 2 compared. In both study areas, healthy trees were never classified as snags. However, there were snags in the field that were misclassified by the algorithm. Snag misclassification was minor in study area 1 and more significant in study area 2.

Table 10. Ground truth field sampling results for both study areas.

Study Area 1				Study Area 2			
Tree #	Species	Ground Truth	Classification	Tree #	Species	Ground Truth	Classification
1	Bw	Snag	Healthy Tree	1	Pj	Snag	Healthy Tree
2	Pj	Snag	Snag	2	Pj	Snag	Snag
3	Pj	Snag	Snag	3	Bw	Snag	Healthy Tree
4	Po	Snag	Snag	4	Pj	Snag	Snag
5	Pj	Snag	Snag	5	Bw	Snag	Healthy Tree
6	Bf	Healthy Tree	Healthy Tree	6	Pj	Healthy Tree	Healthy Tree
7	Pj	Healthy Tree	Healthy Tree	7	Bf	Healthy Tree	Healthy Tree
8	Pj	Healthy Tree	Healthy Tree	8	Po	Healthy Tree	Healthy Tree
9	Po	Healthy Tree	Healthy Tree	9	Bw	Healthy Tree	Healthy Tree
10	Po	Healthy Tree	Healthy Tree	10	Pj	Healthy Tree	Healthy Tree
Snag Accuracy:			80%	Snag Accuracy:			40%
Healthy Tree Accuracy:			100%	Healthy Tree Accuracy:			100%
Total Accuracy:			90%	Total Accuracy:			70%

5.0 DISCUSSION

5.1 SEGMENTATION

Using an optimal set of segmentation parameters is critical for achieving an effective OBIA, as the segmentation is the basis of the process. Each segment is considered an object, so refining them to best fit tree crowns was thought to be necessary. Based on the results in Figures 3 and 4, using the default segmentation parameters provides smaller segmentations that can better capture smaller objects such as delimbed snags. Based on trial and error with qualitative judgement, the parameters used for the OBIA in this study provided larger segmentations that better fit the size and shape of individual tree crowns. By refining these parameters, it reduces the likelihood of non-snag surfaces such as small defoliated portions of healthy trees being identified as a snag.

The parameters used for the segmentation process are evidently both landscape and application dependent. The landscape being assessed is a leading factor in how the parameters should be set, as the shape and size of the average tree crown must be considered. Additionally, it must be considered whether the goal of the application is to identify all snags, or only high hazard/quality snags. The selected segmentation parameters for OBIA in this study were discovered to be best suited for high hazard/quality snag detection. This is due to several small, delimbed snags being too small to be considered their own objects. However, these particular snags pose relatively little risk to the public based on the hazard tree identification guidelines from Fink (2009), so excluding them allows for the classification to be focused on exclusively snags that have higher potential of posing a public hazard; ie. larger, heavier trees with

weakened branches that would cause significant damage or harm. The default segmentation parameters are likely to be sufficient for classifying all snag qualities, though they are subject to errors such as misclassifying fallen timber as snags due to a lack of crown shape definition. Ultimately, the segmentation parameters should be set to meet the goals of the particular application but increasing the number of segmentations and decreasing their sizes may result in increasing the potential for classification errors, which would reduce the overall accuracy.

5.2 CLASSIFICATION & ACCURACY ASSESSMENT

Figures 5-7 evidently show that snags in each study area could be identified using the provided methods. Visually, it is apparent that the density of large snags is greater in study area 1, as there are fewer and more dispersion in study area 2. It can also be noticed that the identification of some snags is not perfect largely due to the segmentation, where some snags only have small portions detected or the detection exceeds the bounds of the snag. Although this is not perfect, it still achieves the goal of locating the position of the snag without considering shape.

It is worth mentioning that the classification algorithm was successful in differentiating fallen timber on the ground from a dead standing tree. Figure 7 makes this apparent, with several downed trees being dispersed and none being classified as a snag. Differentiation between fallen trees and snags was considered as a potential limitation due to reflectance of the surfaces being similar. The effective differentiation was likely achieved by the adjusted

segmentation parameters that produced relatively large segments over downed trees, allowing these objects to blend in as forest ground.

Evidence of misclassifications can be seen in Figures 5 and 7. When looking at the parking lot in Figure 5, it can be noticed that a small portion of a white car has been misclassified as a snag. This is likely the result of the reflectance on that portion of the car being similar to that of the sampled snags. In the upper right portion of Figure 7, it can be noticed that there is a snag that was not classified as one. Although it is a relatively smaller snag, it is still large enough that it was expected to be detected by the algorithm. These instances of misclassification could be results of segmentation, fuzziness, and/or orthomosaic imperfections. Figure 8 shows a particular instance where orthomosaic imperfections was the major contributing factor for misclassification. Although a relatively high frontal and side overlap of 80% was used in flight, further increasing the overlap would help reduce orthomosaic imperfections.

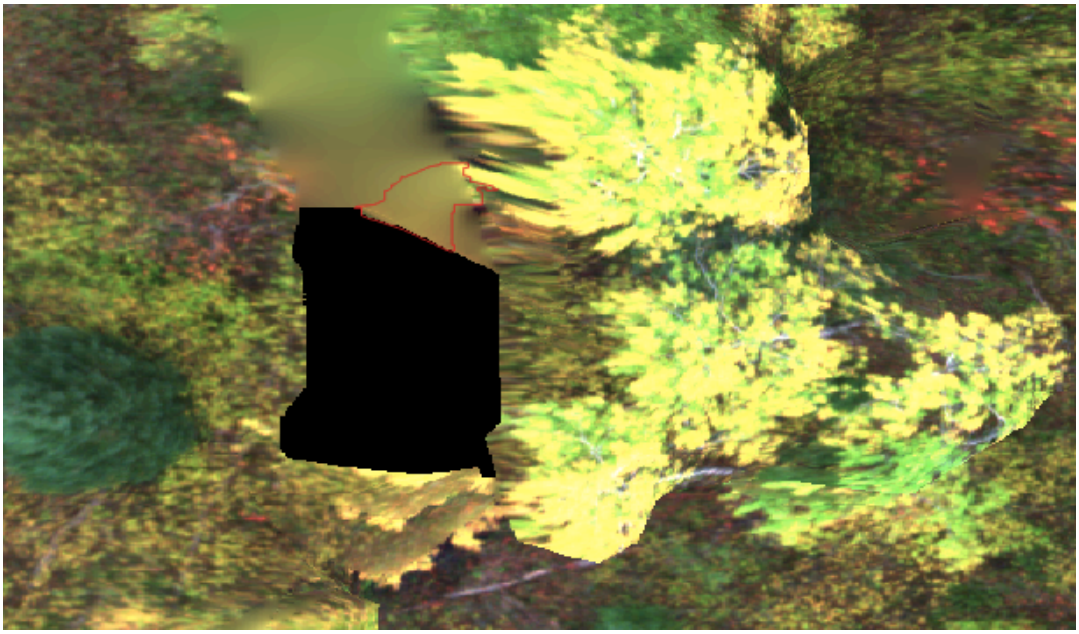

Figure 8. Orthomosaic imperfection resulting in misclassified snag.

The classification results are verified as being accurate in Table 9, with an overall accuracy of 93.4% and a kappa statistic of agreement of 0.87. The user accuracy and producer accuracy of each class are essentially inverses of one another which can be explained by only 2 classes existing, causing every misclassification in one class to affect the accuracy of itself and the other class. Overall, 89.9% being the lowest producer accuracy and 89.0% being the lowest user accuracy proves that high hazard/quality snags can be distinguished in forests with a relatively high degree of accuracy by using these methods.

5.3 FIELD GROUND TRUTH

The results of the field ground truth show that there was a significant difference in accuracy of detecting snags between the two study areas, with study area 1 being 40% more accurate. A major contributing factor to the low accuracy in study area 2 was a poor selection of sample snag trees for the selected classification algorithm. This can only be attributed to human error, as at the time of in-field ground truth sampling, random selection was based on all snags but not necessarily high hazard/quality snags. Figure 9 shows examples of the snags that were not detected by the algorithm in study area 2. It can be seen that these individuals are delimbed and lack any crown, making them low risk snags. Furthermore, between both study areas, white birch was the only snag species that was never successfully classified. This can also be explained by the selection of all white birch snag field samples being individuals that lacked crowns and limbs.

Another potential reason for error in results was the difference in time of when the flight occurred and when the field sampling occurred. There was about a 2-month gap between these tasks, with the flight being around the start of fall and the field sampling being around mid-late fall. This resulted in deciduous foliage being present at the time of flight, but absent at the time of field sampling. An example of where this error may have occurred would be tree #3 in study area 2, which can be seen in Figure 10. The main stem of the tree can be seen as recently snapped but still containing all its foliage, making it unclear whether it is dead or not to the algorithm. By the time the field sampling occurred, this tree was randomly selected as it was visually an obvious snag.

One issue that arose during this process was that some GPS points were not 100% accurate and had deviations by up to a few metres. Low positional accuracy of the GPS unit could have been caused by there being overcast in the sky and/or the antenna being overly obstructed by brush or branches, as the issue mainly occurred for healthy trees. The issue was easily reconciled by using photos and field notes of each individual taken at the time of field sampling and memory of their approximate locations.

Figure 9. Examples of undetected snags in study area 2 (A: Tree #1, B: Tree #5).

Figure 10. Tree #3 in study area 2 (A: orthomosaic view, B: field ground truth view).

5.4 UNSUCCESSFUL APPLICATION OF VEGETATION INDICES

As stated in the objective, it was expected that the application of vegetation indices would be necessary for achieving an accurate detection method. However, this process was excluded from the methods section due to the classification results of the vegetation index rasters being significantly inaccurate and proven unnecessary.

The calculated NDRE index provided a raster that made it difficult to distinguish many trees from forest ground and made healthy trees closer resemble unhealthy trees. The calculated NDVI provided results with healthy trees, unhealthy/snag trees, and forest ground better distinguished. However, due to the season being early autumn at the time of flight, many deciduous trees had already undergone colour changing processes within their leaves. Since the NDVI results were based on the health of foliage it provided inaccurate results, as healthy trees with yellow to red foliage would be detected as a snag. It is possible that a calculated NDVI raster could increase the accuracy of snag detection, so long as the season of flight is when the average tree is foliated with healthy leaves.

5.5 POTENTIAL USE CASES FOR RESULTS

The methods used in this study should only be replicated with the purpose of detecting potentially high hazard snags or high-quality snags. If the goal is to detect all snags then the methods can be followed for reference, although more orthomosaic and OBIA parameter refining will be necessary.

It is clear that these methods would be useful for efficiently detecting potential hazard trees within outdoor recreational/conservation areas. However, detected hazard trees still require in-field visual assessments to verify severity of hazards and make management decisions. This is due to the visuals provided by the orthomosaic not being sufficient enough to accurately verify all aspects of hazard, especially in comparison with what can be assessed in the field. Nonetheless, having access to a digitized spatial reference for hazard trees expedites the detection process and aids in the confirmation of all hazard trees being assessed.

The methods used can also hold value to forest resource managers during operational planning. Operational planners can efficiently spatially assess a harvest block for high quality snags that are valuable to a variety of wildlife and insect species. Managers can then acquire information on the quantity and quality of snags along with their relative coordinates. This snag information could be utilized for making management decisions such as the selection of specific residual snags for the harvested block that would promote biodiversity.

5.6 ADDITIONAL FACTORS TO CONSIDER IN FUTURE STUDIES

The first factor to consider in future studies related to this topic is whether or not the results are dependent on the utilization of a 10-band multispectral sensor. The mean and standard deviation data from all 10 bands were utilized in this study, but it could be possible that the data from a 5-band or even an RGB sensor could be sufficient for classification. Understanding the limitations of the sensors that can be applied to these methods is important, as it could allow

these detection methods to be applied in scenarios where only inexpensive equipment is available.

Another factor to consider is how the classification results would be affected if the data collection flight occurred in the winter season. During the winter, the hardwood trees captured by the sensor would lack foliage. This would effectively make the classification of hardwood snags more difficult than that of coniferous snags. To detect differences between defoliated healthy hardwoods and dead standing hardwoods, the use of vegetation indices would be necessary. Since live trees would have significantly higher water content frozen within their stems in comparison to snags, it is possible that a vegetation index related to water content would be applicable.

Finally, the possibility of an additional classification for unhealthy trees would add significant value to the results found in this study. Although high-quality snags are typical to be considered hazards, individual trees in poor health or structural condition can also potentially be hazardous. Furthermore, the additional class would provide land managers with the ability to spatially assess for individual trees or stands that are experiencing signs of pathogen or insect disturbance, which can be vital for proactive management that is efficient and effective. However, implementation of an unhealthy tree class would require vegetation indices to be applied since more complex spectral signatures must be analyzed, and simple assumptions such as leaf-on versus leaf-off would not be a sufficient basis of health status. High variability within the class may also exist as a result of large quantities of different pathogens and insects existing with varying effects on tree health.

5.7 RECOMMENDATIONS TO THE LRCA

The results from this study could be valuable to the LRCA for hazard tree management in the Cascades Conservation Area. The methods utilized could be applied to more portions of the trail network to expand the spatial data of potentially hazardous trees in the area. However, the classification results without any additional data would be sufficient for managing the Forest Trail with more intensive hazard tree strategies, as it is the most accessible and commonly travelled trail.

Recommended next steps for the LRCA include developing a GIS buffer layer around selected paths. The width of buffers should be determined based on the average height of tall trees within the area. Then, all of the detected hazard trees that intersect with the buffer should be visually assessed in the field and have necessary risk management strategies recorded. Although there are financial limitations that exist, a relatively frequent inspection would be beneficial. In the long term, it may be cheaper to allocate resources towards proactive hazard tree management than dealing with a potential lawsuit due to property damage, injury, or death.

6.0 CONCLUSION

In conclusion, the drone-based MicaSense dual 10-band sensor can be feasibly applied to hazard or high-quality snag detection, but not necessarily snag detection at a full scale using the provided methods. It is evident that the methods used can provide accurate detection results in an efficient manner. Resource and conservation managers can effectively apply these methods for a

variety of purposes where records of the location of hazard trees and/or high-quality snags is important.

During the OBIA process, segmentation has major influences on the degree of hazard and quality of snags that the classification can detect. Trial and error is necessary to generate segments that accurately cover the extent of the desired snags, but segments should be limited to reduce the potential of downed trees being misclassified as snags. Additionally, when performing field ground truth sampling, the random selection of snags should be based on the degree of hazard or quality that is expected to be classified. These steps can be anticipated to ensure the desired snags are detected with high accuracy and increase the accuracy of the field ground truth results.

7.0 LITERATURE CITED

Allison, R.S., J.M. Johnston, G. Craig and S. Jennings. 2016. Airborne optical and thermal remote sensing for wildfire detection and monitoring. Sensors 16(8):1310.

Angers, V.A., P. Drapeau and Y. Bergeron. 2010. Snag degradation pathways of four North American boreal tree species. Forest Ecology and Management 259(3):246-256.

Banu, T.P., G.F. Borlea and C. Banu. 2016. The use of drones in forestry. Journal of Environmental Science and Engineering B 5(11):557-562.

Bannari, A., D. Morin, F. Bonn and A. Huete. 1995. A review of vegetation indices. Remote sensing reviews 13(1-2):95-120.

Bergeron, Y., P.J. Richard, C. Carcaillet, S. Gauthier, M. Flannigan and Y.T. Prairie. 1998. Variability in fire frequency and forest composition in Canada's southeastern boreal forest: a challenge for sustainable forest management. Conservation Ecology 2(2):1-11.

Cohen, J. 1960. A coefficient of agreement for nominal scales. Educational and psychological measurement 20(1):37-46.

Darvishzadeh, R., C. Atzberger, A.K. Skidmore and A.A. Abkar. 2009. Leaf Area Index derivation from hyperspectral vegetation indices and the red edge position. International Journal of Remote Sensing 30(23):6199-6218.

Dash, J.P., G.D. Pearse and M.S. Watt. 2018. UAV multispectral imagery can complement satellite data for monitoring forest health. Remote Sensing 10(8):1216.

Dandois, J.P. and E.C. Ellis. 2013. High spatial resolution three-dimensional mapping of vegetation spectral dynamics using computer vision. Remote Sensing of Environment 136:259-276.

Delegido, J., J. Verrelst, C.M. Meza, J.P. Rivera, L. Alonso and J. Moreno. 2013. A red-edge spectral index for remote sensing estimation of green LAI over agroecosystems. European Journal of Agronomy 46:42-52.

Felderhof, L. and D. Gillieson. 2011. Near-infrared imagery from unmanned aerial systems and satellites can be used to specify fertilizer application rates in tree crops. Canadian Journal of Remote Sensing 37(4):376-386.

Fernández, C.I., B. Leblon, A. Haddadi, K. Wang and J. Wang. 2020. Potato late blight detection at the leaf and canopy levels based in the red and red-edge spectral regions. Remote Sensing 12(8):1292.

Fink, S. 2009. Hazard tree identification by visual tree assessment (VTA): Scientifically solid and practically approved. Arboricultural Journal 32(3):139-155.

Frolking, S., M.W. Palace, D.B. Clark, J.Q. Chambers, H.H. Shugart and G.C. Hurtt. 2009. Forest disturbance and recovery: A general review in the context of spaceborne remote sensing of impacts on aboveground biomass and canopy structure. Journal of Geophysical Research: Biogeosciences 114(G2):1-27.

Getzin, S., K. Wiegand and I. Schöning. 2012. Assessing biodiversity in forests using very high-resolution images and unmanned aerial vehicles. Methods in ecology and evolution 3(2):397-404.

Isgró, M.A., M.D. Basallote and L. Barbero. 2021. Unmanned aerial system-based multispectral water quality monitoring in the Iberian Pyrite Belt (SW Spain). Mine Water and the Environment 40(4):1-12.

Koh, L.P. and S.A. Wich. 2012. Dawn of drone ecology: low-cost autonomous aerial vehicles for conservation. Tropical conservation science 5(2):121-132.

Lefsky, M.A., W.B. Cohen, G.G. Parker and D.J. Harding. 2002. Lidar remote sensing for ecosystem studies: Lidar, an emerging remote sensing technology that directly measures the three-dimensional distribution of plant canopies, can accurately estimate vegetation structural attributes and should be of particular interest to forest, landscape, and global ecologists. BioScience 52(1):19-30.

Lisein, J., M. Pierrot-Deseilligny, S. Bonnet and P. Lejeune. 2013. A photogrammetric workflow for the creation of a forest canopy height model from small unmanned aerial system imagery. Forests 4(4):922-944.

LRCA. n.d. About the LRCA. LRCA. https://lakeheadca.com/about. October 20, 2021.

LRCA. 2016. Cascades Conservation Area Brochure. LRCA. https://lakeheadca.com/application/files/7014/6824/8512/2016_Cascades_Brochure.pdf. November 18, 2021.

LRCA. n.d. HAZARD TREE PROGRAM. LRCA. https://lakeheadca.com/conservation/hazard-tree-program. April 9, 2022.

LRCA. n.d. SUPERIOR STEWARDS. LRCA. https://lakeheadca.com/stewardship/superior-stewards. April 9, 2022.

Mahajan, U. and B.R. Bundel. 2016, October. Drones for normalized difference vegetation index (NDVI), to estimate crop health for precision agriculture: A cheaper alternative for spatial satellite sensors. In Proceedings of the International Conference on Innovative Research in Agriculture, Food Science, Forestry, Horticulture, Aquaculture, Animal Sciences, Biodiversity, Ecological Sciences and Climate Change (AFHABEC-2016), Delhi, India. 22.

MicaSense. 2018. Trifold Dual Camera Product Sheet. MicaSense Inc. https://1w2yci3p7wwa1k9jjd1jygxd-wpengine.netdna-ssl.com/wp-content/uploads/2019/11/Trifold-Dual-Camera-Product-Sheet.pdf. Sept. 30, 2021.

Minařík, R. and J. Langhammer. 2016. Use of a multispectral UAV photogrammetry for detection and tracking of forest disturbance dynamics. International Archives of the Photogrammetry, Remote Sensing & Spatial Information Sciences 41(8):711-718.

Mutanga, O. and A.K. Skidmore. 2007. Red edge shift and biochemical content in grass canopies. ISPRS Journal of Photogrammetry and Remote Sensing 62(1):34-42.

Pasher, J. and D.J. King. 2009. Mapping dead wood distribution in a temperate hardwood forest using high resolution airborne imagery. Forest Ecology and Management 258(7):1536-1548.

Pranga, J., I. Borra-Serrano, J. Aper, T. De Swaef, A. Ghesquiere, P. Quataert, I. Roldán-Ruiz, I.A. Janssens, G. Ruysschaert and P. Lootens. 2021. Improving Accuracy of Herbage Yield Predictions in Perennial Ryegrass with UAV-Based Structural and Spectral Data Fusion and Machine Learning. Remote Sensing 13(17):3459.

Purevdorj, T.S., R, Tateishi, T. Ishiyama and Y. Honda. 1998. Relationships between percent vegetation cover and vegetation indices. International journal of Remote Sensing 19(18):3519-3535.

Risbøl, O. and L. Gustavsen. 2018. LiDAR from drones employed for mapping archaeology–Potential, benefits and challenges. Archaeological Prospection 25(4):329-338.

Rondeaux, G., M. Steven and F. Baret. 1996. Optimization of soil-adjusted vegetation indices. Remote Sensing of Environment 55(2):95-107.

Samiappan, S., L. Hathcock, G. Turnage, C. McCraine, J. Pitchford and R. Moorhead. 2019. Remote sensing of wildfire using a small unmanned aerial system: Post-fire mapping, vegetation recovery and damage analysis in Grand Bay, Mississippi/Alabama, USA. Drones 3(2):43.

Sedykh, V.N. 1995. Using aerial photography and satellite imagery to monitor forest cover in western Siberia. Water, Air, and Soil Pollution 82(1):499-507.

Slaton, M.R., E. Raymond Hunt Jr and W.K. Smith. 2001. Estimating near-infrared leaf reflectance from leaf structural characteristics. American journal of botany 88(2):278-284.

Smiley, E.T., B.R. Fraedrich and P.H. Fengler. 2000. Hazard tree inspection, evaluation, and management. In Handbook of urban and community forestry in the Northeast (pp. 243-260). Springer, Boston, MA. 444.

Stereńczak, K., B. Kraszewski, M. Mielcarek and Ż. Piasecka. 2017. Inventory of standing dead trees in the surroundings of communication routes–The contribution of remote sensing to potential risk assessments. Forest ecology and management 402:76-91.

Tang, L. and G. Shao. 2015. Drone remote sensing for forestry research and practices. Journal of Forestry Research 26(4):791-797.

Thomas, J.W., R.G. Anderson, C. Maser and E.L. Bull. 1979. Snags. In Wildlife habitats in managed forests: the Blue Mountains of Oregon and Washington (pp. 60-77). U.S. Department of Agriculture, Washington, DC. 512.

Wing, B.M., M.W. Ritchie, K. Boston, W.B. Cohen and M.J. Olsen. 2015. Individual snag detection using neighborhood attribute filtered airborne lidar data. Remote Sensing of Environment 163:165-179.

Xiao, Q. and E.G. McPherson. 2005. Tree health mapping with multispectral remote sensing data at UC Davis, California. Urban Ecosystems 8(3):349-361.

Xue, J. and S. Baofeng. 2017. Significant Remote Sensing Vegetation Indices: A Review of Developments and Applications. Journal of Sensors 2017:1353691

Zarco-Tejada, P.J., R. Diaz-Varela, V. Angileri and P. Loudjani. 2014. Tree height quantification using very high resolution imagery acquired from an unmanned aerial vehicle (UAV) and automatic 3D photo-reconstruction methods. European Journal of Agronomy 55:89-99.